Structures 59 (2024) 105693

Contents lists available at ScienceDirect

Structures

journal homepage: www.elsevier.com/locate/structures

Explainable machine learning-aided efficient prediction model and software tool for bond strength of concrete with corroded reinforcement

Tadesse G. Wakjira [a], Abdelrahman Abushanab [b], M. Shahria Alam [a], Wael Alnahhal [b,*], Vagelis Plevris [b]

[a] School of Engineering, Univ. of British Columbia, Kelowna, BC V1V 1V7, Canada
[b] Department of Civil and Environmental Engineering, College of Engineering, Qatar University, P.O. Box 2713, Doha, Qatar

ARTICLE INFO

Keywords:
Machine learning
Bond strength
Concrete
Corrosion
SHAP
Graphical user interface

ABSTRACT

The bond strength between concrete and reinforcement is crucial for the composite action and serviceability of reinforced concrete (RC) structures. However, it is vulnerable to deterioration from the corrosion of reinforcement bars, especially in marine structures. Thus, a precise and reliable model for the bond strength in corrosive environments is necessary to evaluate the serviceability and structural performance of corroded RC members. This study employs explainable machine learning (ML) techniques to assess the bond strength between concrete and corroded bars. Eight ML models are developed to establish the best predictive model for bond behavior, considering seven input parameters: corrosion level (C_L), steel yield strength, compressive strength of concrete, concrete cover-to-bar diameter ratio, bar diameter-to-bonded length ratio, reinforcement type, and test type. The super learner (SL) model, integrating three ML models, outperforms other models and analytical methods with a large R^2 value (98% on the test set) and minimal statistical errors. The SHapley Additive exPlanation (SHAP) technique identifies C_L as the most influential parameter on bond strength, while the reinforcement and test types have the least effect. Finally, a user-friendly graphical user interface (GUI) tool is established to facilitate the practical implementation of the developed model and support accurate bond strength prediction in concrete with steel reinforcement under corrosive environments.

1. Introduction

The bond strength of concrete with reinforcement has a critical impact on the members' composite action and ductility of reinforced concrete (RC) components, which govern the structural performance of structures [1,2]. Furthermore, the robustness of the interaction between steel reinforcement and concrete ensures an effective distribution of tensile stresses between the two materials [3,4]. Nonetheless, the efficiency of the bond strength of RC elements serving in marine environments is at risk of being diminished by steel corrosion, as the concrete cover experiences corrosion-induced cracks, and the reinforcing bars encounter destruction in their cross-sectional areas and ribs, which, in turn, disturb the concrete-steel interface [5]. Such bond degradation raises concerns about the structural behavior, safety, and lifespan of RC buildings with corrosion [6]. Therefore, the assessment of the effectiveness of the bond behavior in corrosive environments is imperative.

The bond strength of RC elements is typically composed of three components: friction, adhesion, and mechanical interlock, which are significantly influenced by steel corrosion [1]. Slight corrosion of steel reinforcement can increase the concrete confinement at the steel-concrete interface, which might increase the contribution of the friction force. However, the rebars' ribs and concrete surface degrade with the corrosion expansion, decreasing the contact surface and friction effect. Additionally, the corrosion process causes a change in the surface of the reinforcement from Fe (iron) to Fe_2O_3 (iron oxide). This effect, coupled with corrosion-induced pressure, can deteriorate the interface, and thus reduce the adhesion contribution. The mechanical interlock is also affected by the deterioration of the bars' ribs and a reduction in concrete compressive strength by the corrosion-induced cracks [1,2].

Numerous experimental investigations have been performed on the bond strength between corroded steel bars and concrete [7–10,2]. Al-Sulaimani et al. [7] and Abushanab and Alnahhal [2] observed that the bond strength decreased by about 50% at a corrosion level (C_L) between 6% and 10%. A similar result was reported in the study by Zhao

* Corresponding author.
E-mail address: wael.alnahhal@qu.edu.qa (W. Alnahhal).

https://doi.org/10.1016/j.istruc.2023.105693
Received 8 May 2023; Received in revised form 30 October 2023; Accepted 2 December 2023
Available online 18 December 2023

Table 1
Descriptive statistics of the input parameters.

Factors	Mean	Standard deviation	Minimum	Quartiles			Maximum
				First	Second	Third	
f_c (MPa)	32.38	10.20	22.13	23.00	30.00	34.00	52.10
f_y (MPa)	448	63	290	389	458	500	606
C_L (%)	4.39	4.12	0.10	1.40	3.30	5.56	18.75
c_c/d_b	3.10	1.66	0.78	1.90	3.00	4.18	5.90
d_b/l_b	0.20	0.06	0.04	0.15	0.17	0.28	0.28
Reinforcement type	Deformed bars, smooth bars						
Test type	Beam specimen, pull-out specimen						

et al. [8]. In addition, Al-Sulaimani et al. [7] reported that corroded specimens with greater concrete cover thickness exhibited higher bond strength. Lin and Zhao [9] observed that corrosion changed the bond failure mode from concrete shearing between steel lugs to frictional slippage. Several analytical formulations have also been established to predict the concrete-steel bond strength under a corrosive environment [11–13]. However, they are empirically derived based on limited database and important factors, which limits their prediction capability. Moreover, a nonlinear and complex relationship exists between the bond strength and its predictor parameters due to the inherent uncertainties related to steel bar type, corroding environment, concrete cover thickness, corrosion methods and levels, concrete and reinforcement properties, and members' geometry [14]. Therefore, it is vital to develop an accurate and reliable bond strength prediction model.

Recently, machine learning (ML) models have shown to be promising in modeling different civil engineering problems [15-21]. Such models have the ability to establish the relationship between input and output variables without requiring prior knowledge of the governing physical or mathematical models. Consequently, different ML models have been investigated to evaluate the performance of RC elements [22–28]. However, few studies have evaluated the efficacy of ML algorithms for modeling the bond strength between steel and concrete [5,14,29,30]. Dahou et al. [31] constructed an ANN model to predict the bond strength of concrete using a dataset of 112 bond strength results, considering only two factors: steel bar diameter and concrete mix. Golafshani et al. [32] utilized ANN and fuzzy logic to predict the bond strength of spliced steel bars based on 179 spliced beam samples. Hoang et al. [5] employed the least squares support vector regression and differential flower pollination methods to construct a model for the bond strength under the effect of corrosion using a database of 218 test results. However, these models neglect important factors such as concrete cover-to-bar diameter (c_c/d_b) and bar diameter-to-bonded length (d_b/l_b) ratios that have shown to have significant effects on the bond strength [13,33,34]. For instance, concrete cover has a direct relation with the reinforcing bars, especially in corrosive environments. With a higher concrete cover, more protection is provided for steel reinforcement against corrosion and thus less bar diameter degradation and better bond strength is achieved [2]. Nevertheless, to date, no study has examined the simultaneous effect of steel yield strength, compressive strength of concrete, reinforcement type, C_L, c_c/d_b ratio, d_b/l_b ratio, and test type on the bond strength between concrete and reinforcement.

Moreover, previous studies primarily focused on developing ML models without addressing their practical application. Therefore, this study aims to develop an accurate and reliable ML-based predictive model for the bond strength between concrete and corroded steel reinforcement. The study also aims to establish a user-friendly predictive software tool for the practical implementation of the developed ML model. To accomplish this, a database of 249 experimental results on bond strength of concrete with corroded reinforcement was compiled from previous studies [9,12,13,35,36–43]. The dataset was then pre-processed and randomly split into training (80%) and test (20%) sets. Different ML models, ranging from rather simple (classification and regression tree (CART), kernel ridge regression (KRR), support vector regression (SVR), k-nearest neighbors (kNN)) to advanced complex ones (adaptive boosting (ADB), gradient boosting tree (GBT), extreme gradient boosting (xgBoost)), are trained on the training dataset and evaluated using the test dataset with the aim of developing an accurate and efficient predictive model. Apart from these models, the current study developed a novel advanced super-learner model with the aim to develop an accurate and reliable predictive model. Three predictive models are integrated in a super-learner model to improve their efficacy in predicting bond strength. The accuracy of the proposed SL model was then evaluated by comparing its predictive capability with the existing bond strength models. Additionally, a unified model-agnostic framework known as the SHapley Additive exPlanation (SHAP) technique was utilized for the first time, to explain the bond strength predictions of the ML model and to rank the input features based on their importance in predicting bond strength. Finally, a graphical user interface (GUI) based, user-friendly, and efficient software tool is developed for the practical application of the developed SL model.

2. Existing analytical models

To evaluate the practicality and reliability of the proposed model, its predictive performance was investigated against the existing analytical models of Cabrera [11], Chung et al. [12], and Stanish et al. [44]. The details of the analytical models are presented in the following subsections.

2.1. Cabrera [11] model

As per Cabrera [11], the bond strength of normal and fly ash concrete can be calculated by Eqs. (1) and (2), respectively:

$$\tau_u = 23.478 - 1.313C_L \tag{1}$$

$$\tau_{uf} = 26.133 - 1.341C_L \tag{2}$$

where τ_u and τ_{uf} are the bond strength of normal and fly ash concrete, respectively.

It can be seen that in both types of concrete, the proposed equations of Cabrera [11] are a function of the corrosion level only, utilizing a simple linear functions.

2.2. Chung et al. [12] model

The bond strength predictive equation of Chung et al. [12] considers two scenarios for the C_L, as presented in Eq. (3):

$$\tau_u = \begin{cases} 16.87, \ for \quad C_L \le 2\% \\ 24.7{C_L}^{-0.55}, \ for \quad C_L > 2\% \end{cases} \tag{3}$$

Similar to Cabrera [11], the prediction model of Chung et al. [12] depends only on the corrosion level of steel, but this time the relationship is not linear for $C_L > 2\%$.

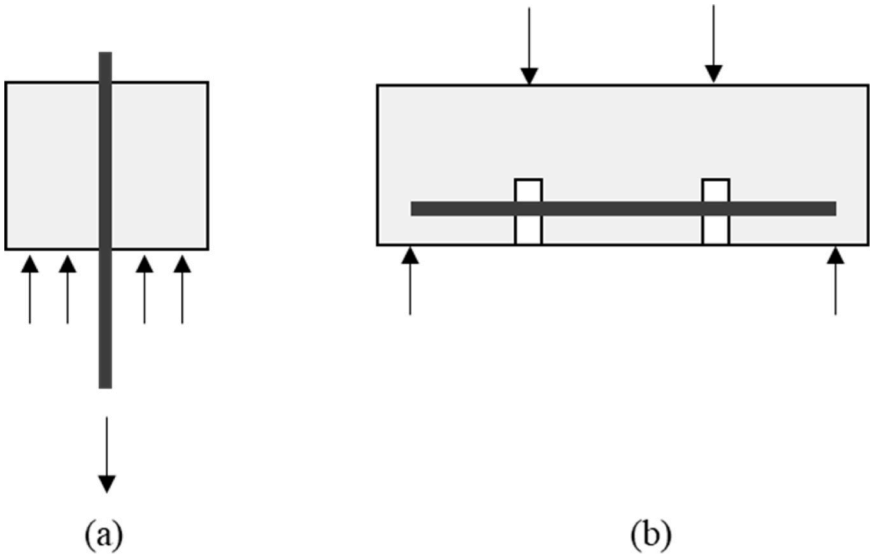

Fig. 1. Test types: (a) pull-out and (b) beam.

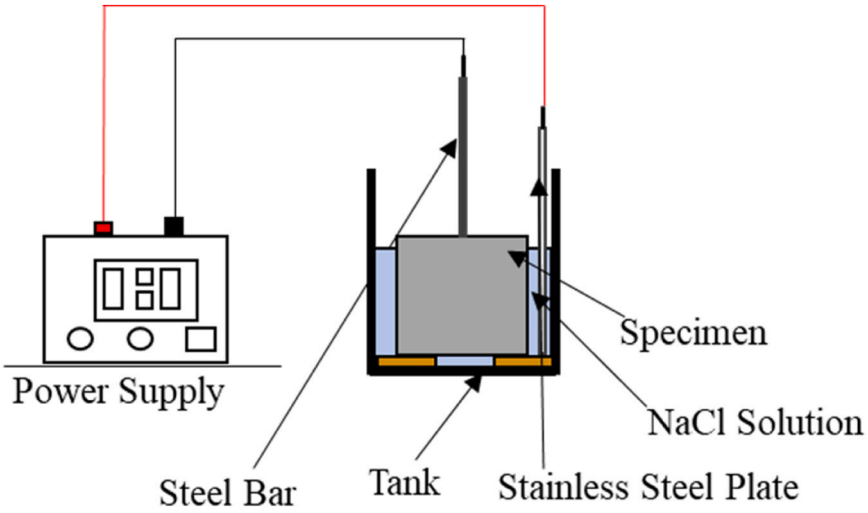

Fig. 2. A schematic of the corrosion setup.

2.3. Stanish et al. [44] model

Unlike the previous two models, Stanish et al. [44] introduced the effect of concrete compressive strength in addition to the steel corrosion level in determining the bond strength. Accordingly, the bond strength of concrete can be estimated using the analytical formula of Stanish et al. [44] as per Eq. (4):

$$\tau_u = (0.77 - 0.027C_L)\sqrt{f_c'} \quad (4)$$

3. Description of the database and input parameters

A comprehensive dataset comprising 249 experimental results pertaining to the bond behavior between concrete and corroded steel bars was compiled from 12 studies found in the literature [9,12,13,35,36–43]. The dataset comprised seven input parameters: (i) corrosion level, (ii) steel yield strength, (iii) compressive strength of concrete, (iv) c_c/d_b ratio, (v) d_b/l_b ratio, (vi) reinforcement type, and (vii) test type (pull-out and beam). A statistical summary of the input parameters is provided in Table 1. The compiled database comprised both numerical and categorical input variables. The reinforcement and test type were categorical variables, whereas the rest were numerical variables. Both deformed and smooth bars have been considered in the database. Moreover, two test types were investigated; namely, beam and pull-out specimens, as illustrated in Fig. 1. The significance of adding this parameter is to cover the available two mechanisms in evaluating the bond strength of concrete, which yield different responses. The specimens in the database were corroded using the electrochemical system. A schematic of the electrochemical corrosion setup is presented in Fig. 2. In all tests, anode, cathode, sodium chloride solution, and power supply were present to accelerate the corrosion process.

4. Description of ML models

To develop powerful and efficient ML-based bond strength predictive models, it is important to explore various ML algorithms, starting from the simplest one and moving on to more complex and advanced ML models. Therefore, eight different ML algorithms have been investigated in the present study, including CART, KRR, SVR, kNN, ADB, GBT, xgBoost, and super learner models. The first four models are single models that are easier to explain and interpret, while ADB, GBT, and xgBoost are ensemble models that integrate several CARTs in series to

develop a stronger model. Super learner further improves the efficacy of the ML models by integrating different ML learners. A brief description of each ML model is provided in the following subsections.

4.1. Single models

As discussed earlier, four single models are considered in this study. The details of the models are as follows:

4.1.1. K-nearest neighbor

K-nearest neighbor often abbreviated as kNN, is a non-parametric supervised learning algorithm that can be used for both classification and regression problems. As its name implies, kNN uses proximity to make predictions. Given training samples $\left\{\left(x_j, y_j\right)\right\}_{j=1}^{n}$ with n number of samples, kNN determines a predefined number of training samples that are nearest in distance to the query point x. The prediction of bond strength at the query point is then determined as the weighted mean of the bond strength for the K training samples that are closest to x. The neighbor size K should be optimized to obtain the best predictive kNN model.

4.1.2. Kernel ridge regression

Kernel ridge regression, or KRR for short, utilizes kernel technique and regularization to make predictions. It combines ridge regression with kernel trick to mitigate the drawbacks of the popular least square method. Nonlinear kernel functions are used to transform nonlinear regression in the original space into a linearly separable space in a higher dimensional space. The commonly used nonlinear kernel functions include polynomial, radial basis function (RBF), and sigmoid (hyperbolic tangent) kernel functions [45].

4.1.3. Support vector regression

Support vector regression is a supervised ML model in which a unique prediction is obtained based on structural risk optimization, which can be used to solve multidimensional nonlinear problems with medium or small training datasets. Similar to KRR, SVR uses kernel function to map the original sample space into a higher dimensional space where they can be linearly separable. Given the training set $\left\{\left(x_j, y_j\right)\right\}_{j=1}^{n}$ with n number of samples, where $x_j \epsilon \mathbb{R}^M$ is the input vector, $y_j \epsilon \mathbb{R}$ is the response variable, and M is the dimension of the input vector, the final solution of SVR can be given by Eq. (5) in terms of the kernel function, $K(x_i, x)$, regularization parameter, C, and bias b.

$$f(x) = \sum_{i \epsilon SV} \left(\alpha_i - \alpha_i^*\right) K(x_i, x) + b \tag{5}$$

Here, $\alpha_i, \alpha_i^{'} \epsilon [0, C]$ are Lagrange multipliers of the lower and upper support vectors (SV), which are subsets of the training samples.

4.1.4. Classification and regression tree

Classification and regression tree is a supervised learning algorithm that mimics the tree structure with random numbers of nodes and branches. CART is composed of a root node, which represents the most important factor, internal nodes that correspond to the characteristics of the training dataset, and the terminal (leaf) node that denotes the predicted response variable (bond strength in this study). The key hyperparameters in CART are maximum depth of the tree, minimum number of samples required to be at a terminal node, number of input features, and minimum number of samples required to split an internal node. The CART model is simple to visualize, understand, and interpret. However, a single tree can be unstable and can suffer from the problem of overfitting. As a result, several CART models can be combined in an ensemble model to overcome the problem of the single CART model and enhance its efficiency.

4.2. Boosting ensemble models

Boosting ensemble models are one of the most effective ML models that can be used for both regression and classification problems. Boosting ensemble models combine a set of base learners (a.k.a. weak learners) sequentially and integrate their results to reduce the overall error and ultimately form a strong and efficient ensemble model. Particularly, a new base learner is added to the boosting ensemble model at each iteration during the learning process, up to a specified limit. Adaptive boosting, gradient boosting tree, and xgBoost are three popular types of boosting ensemble models. Herein, a CART model is employed as the base learner for all the boosting ensemble models.

4.2.1. Adaptive boosting

Adaptive boosting is the first boosting ensemble model that combines weak learners in sequence by assigning different weights to the data that will be used in the next weak learner [46]. Given $\left\{\left(x_j, y_i\right)\right\}_{j=1}^{n}$ training dataset, in the first iteration, ADB assigns the same weight ($\left\{w_j^{(1)} = 1/n\right\}$) to all the training data. In the subsequent iteration(s), the weight distribution is modified to provide more focus to the incorrectly predicted instance by assigning lesser weights to the accurately predicted instances and higher weights to erroneous prediction instances. The weight of the training samples at iteration $i+1$ is determined as follows:

$$w_j^{(i+1)} = \frac{w_j^{(i)} {\beta_i}^{1-L_j^{(i)}}}{\sum_{j=1}^{n} w_j^{(i)} {\beta_i}^{1-L_j^{(i)}}} \tag{6}$$

$$\beta_j = \frac{\overline{L^{(i)}}}{1 - \overline{L^{(i)}}} \tag{7}$$

where $\overline{L^{(i)}} = \sum_{j=1}^{n} L_j^{(i)} w_j^{(i)}$ is the average loss of weak estimator $E^i(X)$ and $L_j^{(i)}$ is the loss function, which can be a linear, square, or exponential.

The key hyperparameter of ADB including the number of estimators (CART), learning rate, maximum depth of the base learner, and the number of features for the base learner are optimized in this study to obtain the best predictive ADB model.

4.2.2. Gradient boosting tree

The gradient boosting algorithm is based on the principle that each base model learns from the residuals of the previous base learner(s). It allows the optimization of arbitrary differentiable loss functions. In each iteration, it fits the basic learner (CART in this study) on the negative gradient of the given loss function. Letting $\left\{\left(x_j, y_i\right)\right\}_{j=1}^{n}$ represent a set of the training data samples, the general algorithm for GBT with T number of estimators can be summarized as follows:

(a) Fit CART estimator E^0.
(b) For i in [1, T]:

- Determine the loss in i^{th} iteration, L^i.
- Compute the negative gradient: $g^i = -\left[\frac{\partial L^i\left(Y_j, E^i\left(X_j\right)\right)}{\partial E^i\left(X_j\right)}\right]$.
- Fit a new CART H^i on $\left(X, g^i\right)$.
- Determine the multiplier ρ^i, where $\rho^i = \underset{\gamma}{\operatorname{argmin}} \sum_j L\left(Y_j, E^{i-1}\left(X_j\right) + \rho H^i\left(X_j\right)\right)$.
- Update the model: $E^i(X) = E^{i-1}(X) + \rho^i H^i(X)$.

(c) Output the final model, $E^T(X)$.

The key hyperparameters of GBT are the number of estimators (CARTs), maximum depth of CART, learning rate, and maximum

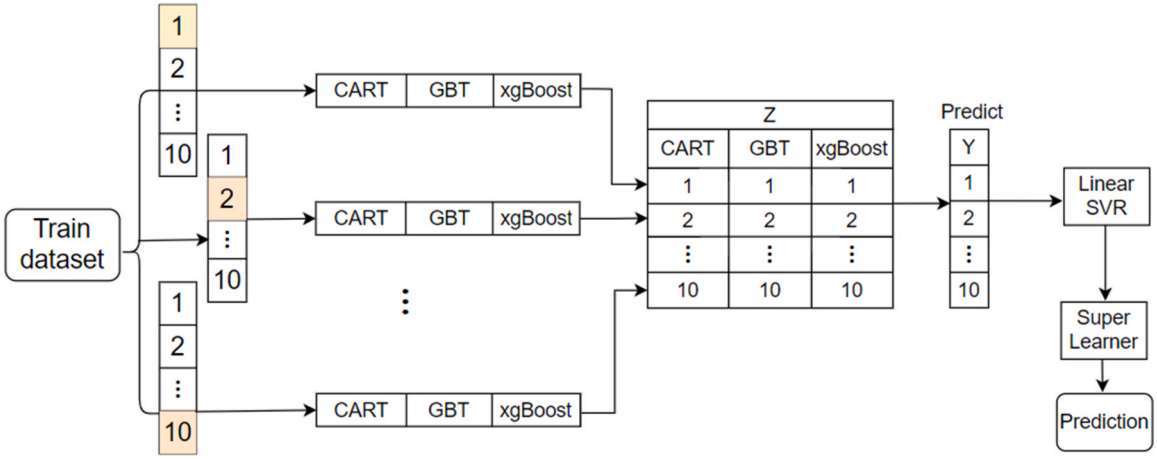

Fig. 3. Proposed super learner model.

number of input features.

4.2.3. Extreme gradient boosting

Extreme gradient boosting is a widely recognized advanced ML algorithm that was developed as an enhanced version of the gradient boosting algorithm [47]. Despite its efficiency relative to other boosting ensemble models, xgBoost is difficult to understand and interpret. Like the gradient boosting algorithm, multiple base learners are integrated sequentially to form a strong model; however, it uses a more generalized formulation to control model complexity and overfitting. A technique referred to as regularization is introduced in xgBoost to mitigate overfitting, which is one of its main advantages over other boosting algorithms. The objective of xgBoost is to minimize the loss function under the condition of minimum complexity of the model. As a result, the objective function, $L(\varphi)$ in xgBoost is composed of the loss function and regularization term, which penalizes model complexity, as shown below [47]:

$$L(\varphi) = \sum_j l\left(y_j, \hat{y}_j\right) + \sum_i \Omega(f_i) \tag{8}$$

$$\Omega(f_i) = \gamma K + \frac{1}{2}\lambda \sum_{i=1}^{K} w_i^2 \tag{9}$$

where l is the loss function, which is used to determine the difference between the actual (y_j) and predicted values ($\hat{y}_j$) of the bond strength, γ is the minimum required loss reduction for splitting a new leaf node, K is the number of leaves, w_j is leave scores, and λ is the penalty coefficient.

4.3. Super learner model

Super learner (SL) determines an optimal prediction of the bond strength by calculating a weighted combination of the predicted bond strength from an ensemble of candidate models [48]. The proposed SL algorithm in this study combines three models; namely, CART, GBT, and xgBoost, as will be discussed in Section 6. The developed model ensures the best combination of the candidate models to produce an efficient model. The weights of the three models are determined using 10-fold cross-validation. Fig. 3 summarizes the learning process in the SL algorithm. In the first step, the original training sample is split into 10 folds. The three models are then evaluated using the 10-fold cross-validation and a matrix Z is constructed using out-of-fold predictions. Finally, a meta-model (linear SVR in this study) fitted on (Z, Y) is used to predict the bond strength, as shown in Fig. 3.

Table 2
Statistical evaluation metrics.

Evaluation metric	Formulation	Perfect match value
Mean absolute error	$MAE = \frac{1}{N}\sum_{i=1}^{N}\lvert y_i - \hat{y}_i\rvert$	MAE = 0
Mean absolute percent error	$MAPE = \frac{1}{N}\sum_{i=1}^{N}\left\lvert\frac{y_i - \hat{y}_i}{y_i}\right\rvert$	MAPE = 0
Root mean squared error	$RMSE = \sqrt{\frac{1}{N}\sum_{i=1}^{N}(y_i - \hat{y}_i)^2}$	RMSE = 0
Relative root mean squared error	$RRMSE = \sqrt{\frac{1}{N}\sum_{i=1}^{N}(y_i - \hat{y}_i)^2}$	RRMSE = 0
Coefficient of determination	$R^2 = 1 - \frac{\sum_{i=1}^{N}(y_i - \hat{y}_i)^2}{\sum_{i=1}^{N}(y_i - \bar{y})^2}$	$R^2 = 1$
Agreement index	$I_A = 1 - \frac{\sum_{i=1}^{n}(y_i - \hat{y}_i)^2}{\sum_{i=1}^{n}(\lvert y_i - \bar{y}\rvert + \lvert\hat{y}_i - \bar{y}\rvert)^2}$	$I_A = 1$
Kling-Gupta efficiency	$KGE = 1 - \sqrt{(r-1)^2 + (\alpha-1)^2 + (\beta-1)^2}$	KGE = 1

5. Optimization and evaluations of the models

Hyperparameter optimization or tuning is an important step in developing machine learning-based models. In this study, grid search is used in conjunction with 10-fold cross-validation in order to optimize the hyperparameters of all ML models. Grid search is an optimization technique that exhaustively searches through a specified subset of the hyperparameter space. The 10-fold cross-validation randomly splits the training data into 10 disjoint groups of equal size, then traverses the 10 groups in turn, each time using the current group for model validation, and all the remaining groups for model training. Finally, the mean of the performance from the ten validation sets is used as the performance of the cross-validated model. In this study, root mean squared error (RMSE) is used as the performance index for selecting the optimal model. The performance of the optimal models is further analyzed and compared using seven statistical evaluation metrics: coefficient of determination (R^2), RMSE, mean absolute percentage error (MAPE), relative root mean squared error (RRMSE), mean absolute error (MAE), Kling Gupta efficiency (KGE), and agreement index (I_A). Utilizing a diverse set of performance metrics ensures a thorough and detailed evaluation of the models. The coefficient of determination gauges how well actual values are replicated by the model, explaining the variance in the response variable. The RMSE quantifies the model's prediction error, providing a sense of accuracy, while MAPE offers insights into the model's accuracy as a percentage, making it easier to interpret in practical scenarios. The RRMSE standardizes the RMSE, enabling comparisons across different datasets or models. The MAE gives an average

Table 3
Optimized hyperparameters of the models.

ML model type	Hyperparameters and Their Optimized Values
KNN	Leaf size: 2; Number of neighbors (k): 2
KRR	Kernel type: radial basis function; Alpha: 0.014
SVR	C: 162; Epsilon: 0.003; Kernel type: radial basis function
CART	Maximum tree depth: 8; Maximum number of features: 5; Minimum samples split: 3
ADB	Base learner: CART; maximum depth of base learner: 9; Maximum features: 3; Number of base learners: 38; Learning rate: 0.2
GBT	Number of base learners: 115; Maximum depth: 7; Learning rate: 0.15; Subsample: 0.4; Maximum features: 3
xgBoost	Number of base learners: 255; Maximum depth: 13; Learning rate: 0.25; Subsample: 0.3; Column sample by level: 0.9; Column sample by node: 0.9; Column sample by tree: 1.0

magnitude of errors between predicted and observed values, without considering direction. KGE captures the simultaneous correlation, bias, and variability between observed and simulated values. Finally, I_A assesses the degree to which predicted values match observed ones, serving as a measure of model accuracy. Table 2 presents the formulations of the seven performance evaluation metrics, where y_i and $\hat{y}_i$ are observed response value and its corresponding predicted value, respectively, r is the linear correlation between y_i and $\hat{y}_i$, α is a measure of variability, and β is the bias. It should be noted that in this work, the R^2 which is calculated using the formula shown in Table 2 is not equal to the square of the Pearson correlation coefficient. For details on the difference between the two, the interested reader is referred to [49].

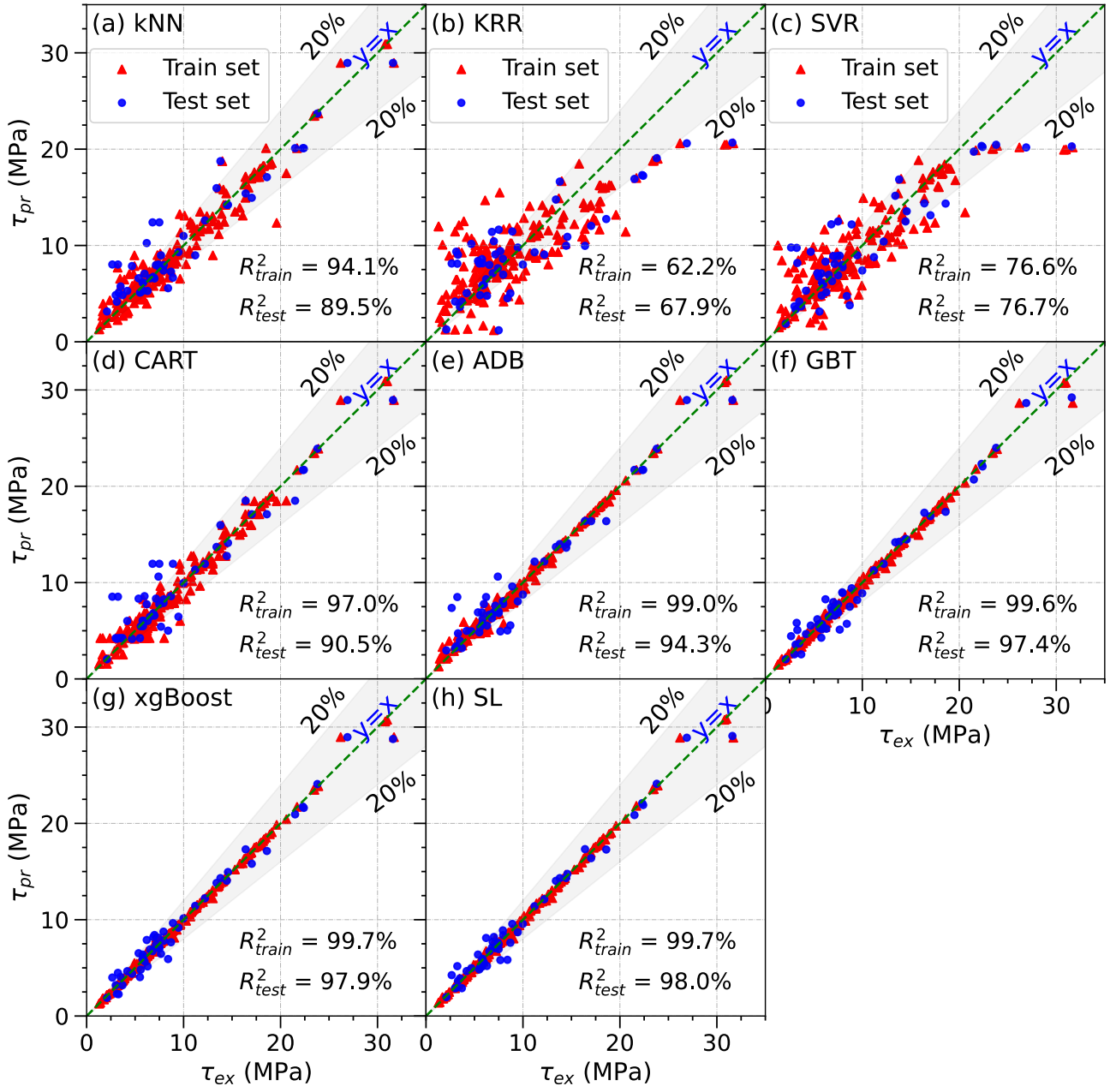

Fig. 4. Comparison of predicted and actual bond strength.

Table 4
Performance measures of the ML models.

Performance index	kNN	KRR	SVR	CART	ADB	GBT	xgBoost	SL
				Train Set				
MAE (MPa)	0.97	2.70	1.92	0.68	0.31	0.23	0.12	0.16
MAPE (%)	15.1	47.4	33.3	11.6	6.17	3.26	1.46	2.08
RMSE (MPa)	1.42	3.58	2.82	1.01	0.58	0.39	0.32	0.33
RRMSE (MPa)	0.15	0.38	0.30	0.11	0.06	0.04	0.03	0.04
R^2 (%)	94.1	62.2	76.6	97.0	99.0	99.6	99.7	99.7
I_A (%)	98.5	86.0	92.3	99.2	99.8	99.9	99.9	99.9
KGE (%)	95.5	63.3	76.0	97.9	98.3	99.1	99.4	99.6
				Test Set				
MAE (MPa)	1.63	3.08	2.40	1.45	1.08	0.83	0.77	0.71
MAPE (%)	26.8	41.4	33.4	23.8	18.6	13.1	11.1	10.2
RMSE (MPa)	2.20	3.85	3.28	2.10	1.62	1.10	0.99	0.96
RRMSE (MPa)	0.23	0.41	0.35	0.22	0.17	0.12	0.10	0.10
R^2 (%)	89.5	67.9	76.7	90.5	94.3	97.4	97.9	98.0
I_A (%)	97.1	87.7	92.0	97.4	98.5	99.3	99.5	99.5
KGE (%)	88.4	63.1	72.8	90.7	94.5	97.9	97.7	98.0

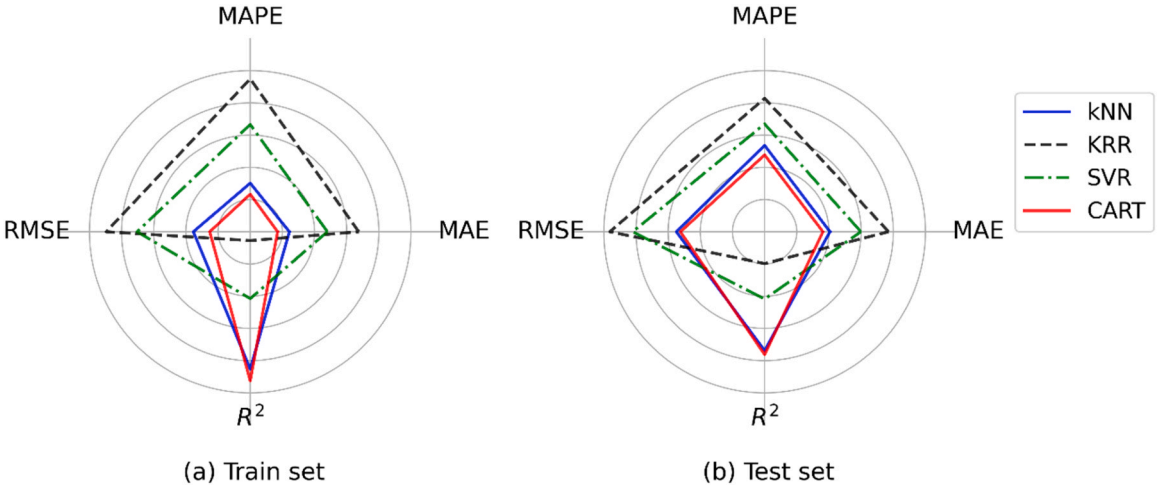

Fig. 5. Performance of single models in predicting bond strength.

6. Results and discussion

6.1. ML model predictions

This section evaluates and compares the prediction capabilities of optimized ML models. Table 3 summarizes the optimized hyper-parameters for each model except SL, while the SL model integrates the optimized CART, GBT, and xgBoost to make predictions. The scatter plots in Fig. 4 show a comparison between the experimental ultimate bond strength (τ_{ex}) and its predicted counterpart (τ_{pr}) using the

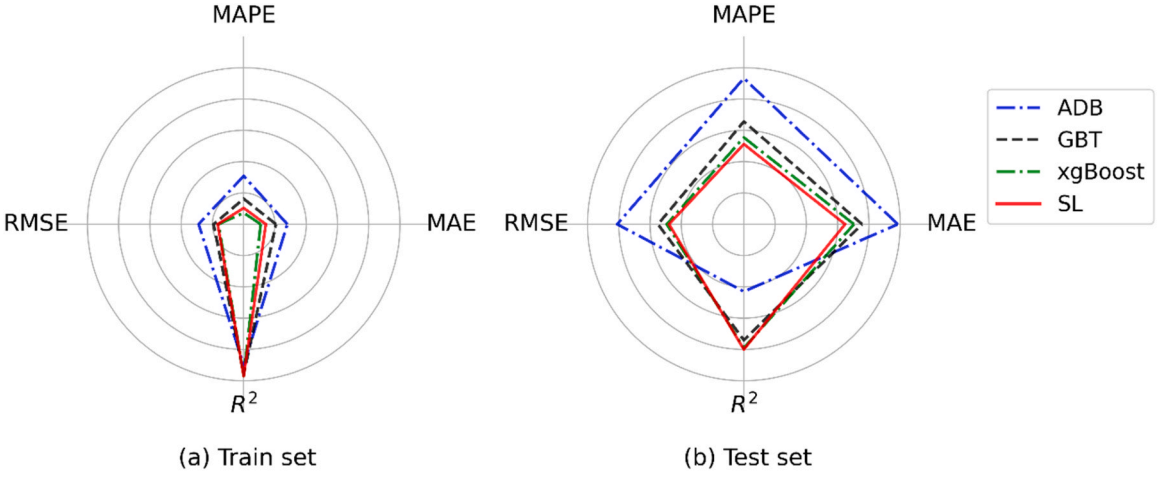

Fig. 6. Performance of ensemble and SL models in predicting bond strength.

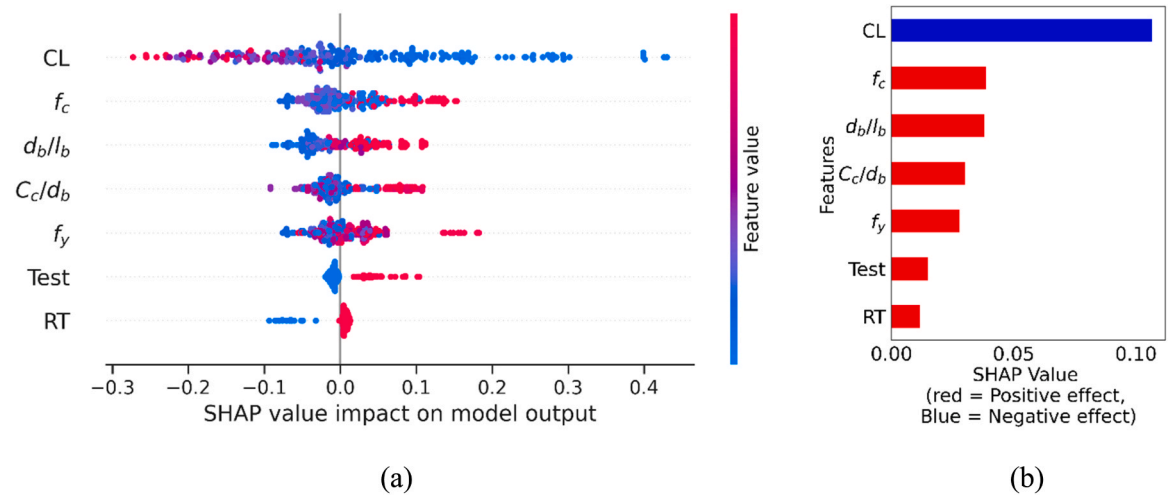

Fig. 7. Summary plot for elucidating the global feature influences of the input features (a) and global importance of the input features (b).

optimized ML models. An equity line with ± 20% error bounds is also provided in each scatter plot to visualize the accuracy and distribution of the data points. It can be seen from the results that the single models have noticeably lower prediction accuracy compared to the ensemble models, evidenced by the models' R^2 values and the scattered point distribution between the error bounds. For the single models, KRR exhibited the least accurate prediction ability with an R^2 of 62.2% and 67.9% on the training and test sets, respectively. Furthermore, CART predictions outperformed all single models with an R^2 of 97% and 90.5% for the training and test sets, respectively. For the ensemble predictions, the results show a good agreement between τ_{ex} and τ_{pr} in terms of R^2, I_A, and KGE. This could be exemplified as the majority of the predicted data by the ensemble models were within the ± 20% error bounds. It can also be noticed that the R^2 on both the training and test datasets of all proposed ensemble models were greater than 94%, implying the effectiveness of the ensemble models in predicting the bond strength of concrete with corroded bars. The prediction accuracy of the models is further improved in the SL model, as evidenced by the highest R^2_{test} of 98%.

Table 4, Fig. 5, and Fig. 6 further demonstrate the prediction capabilities of the models on both the training and test sets in terms of the eight statistical measures; particularly, MAE, MAPE, RMSE, RRMSE, R^2, AI, and KGE. It can be seen that among the investigated models, KRR and SVR models reported the least predictive accuracy, attributable to their high error (MAE, MAPE, RMSE, and RRMSE) and low R^2, AI, and KGE. Table 4 and Fig. 5 also reveal that the CART model had the highest prediction performance among the single models with RRMSE and KGE of 0.11 MPa and 97.9% on the training set and 0.22 MPa and 90.7% on the test set, respectively. On the other hand, all ensemble models yielded higher predictive accuracy than the single models, as listed in Table 4. That is because the ensemble algorithms integrate weak learners of individual algorithms to produce an improved learner with better predictive accuracy. Among the investigated ensemble models, the ADB model achieved the lowest R^2 on the test set (94.3%), as listed in Table 4. Furthermore, it was found that the SL model outperformed all ensemble models on the test set. For example, the SL model had R^2 and RMSE of 98% and 0.96 MPa, while ADB, GBT, had xgBoost showed R^2 and RMSE of 94.3% and 1.62 MPa, 97.4% and 1.10 MPa, and 97.9% and 0.99 MPa, respectively. The accuracy of the SL model relative to other ensemble models in terms of the statistical performance measures can also be observed in Fig. 6.

6.2. Model interpretations

Despite the effectiveness of the proposed model in predicting the bond strength of concrete under corrosive conditions, the high complexity of the model makes it a black box and therefore makes the interpretation of its output difficult, which in turn, limits the utilization of the models in practical applications. Several methods have been employed in the literature to help interpret the outputs of complex ML models; one of which is the SHAP, which has been recently established by Lundberg and Lee [50]. The SHAP technique was developed based on a game theory. In this approach, an important factor or SHAP value is computed for each input factor, and the comparison is made by analyzing the model with and without this factor. Moreover, the SHAP values can be used to prioritize the factors in descending order based on their effect on the response, of which the highest SHAP values are assigned for the most significant factor and vice versa. However, to the best of the authors' knowledge, there has been no previous research on the interpretability and effectiveness of ML models for predicting the bond strength of concrete with corroded bars. Therefore, this study used the SHAP approach to explain the predictions of the bond strength and rank the input features based on their impact on the bond strength.

Fig. 7 illustrates the SHAP summary plot, where the input factors are presented on the *y*-axis in descending order according to their contribution to the bond strength, the most significant factor being placed at the top. The influence of the factors on the model's output is presented on the *x*-axis in terms of the SHAP values. The SHAP values are classified into colored points according to the effect of the factors on the model in Fig. 7(a). Each point represents the effect of a particular factor on an observation from the entire database, where blue represents low factor values and reddish pink represents high factor values (Fig. 7(a)). In addition, the average of absolute SHAP values of each factor is presented in Fig. 7(b) to demonstrate the global importance of the factors on the bond strength of concrete. In Fig. 7(b), the average absolute SHAP values are plotted on the x-axis and the importance of each factor on the bond strength of concrete is shown on the y-axis. The direction and degree of each factor can also be revealed from the same figure, in which factors in blue cause a reduction in the bond strength (negative effect), while those shown in red increase the bond strength of concrete (positive effect). Moreover, bars with higher lengths indicate a higher effect on the bond strength. It can be seen from Fig. 7(b) that the C_L is the most influential factor on the bond strength between concrete and steel bars under corrosive conditions, followed by concrete compressive strength, d_b/l_b, c_c/d_b, steel yield strength, test type, and reinforcement type (RT). It can also be observed that all factors except the C_L have positive effects on the bond strength of concrete, which means the increase in all factors except C_L increases the bond strength, while the increase in C_L reduces the bond strength. Moreover, it can be noticed that deformed steel bars and beam specimens have higher bond strength compared to plain

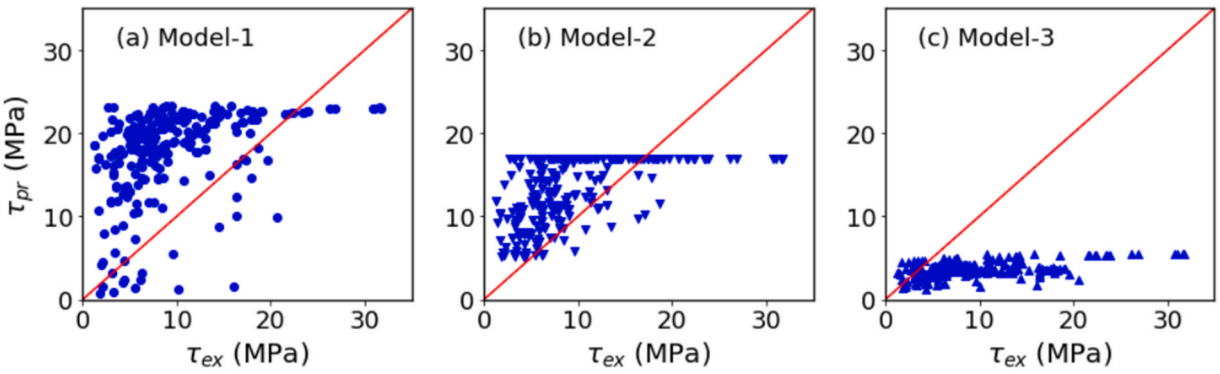

Fig. 8. Experimental versus predicted bond strength based on existing models.

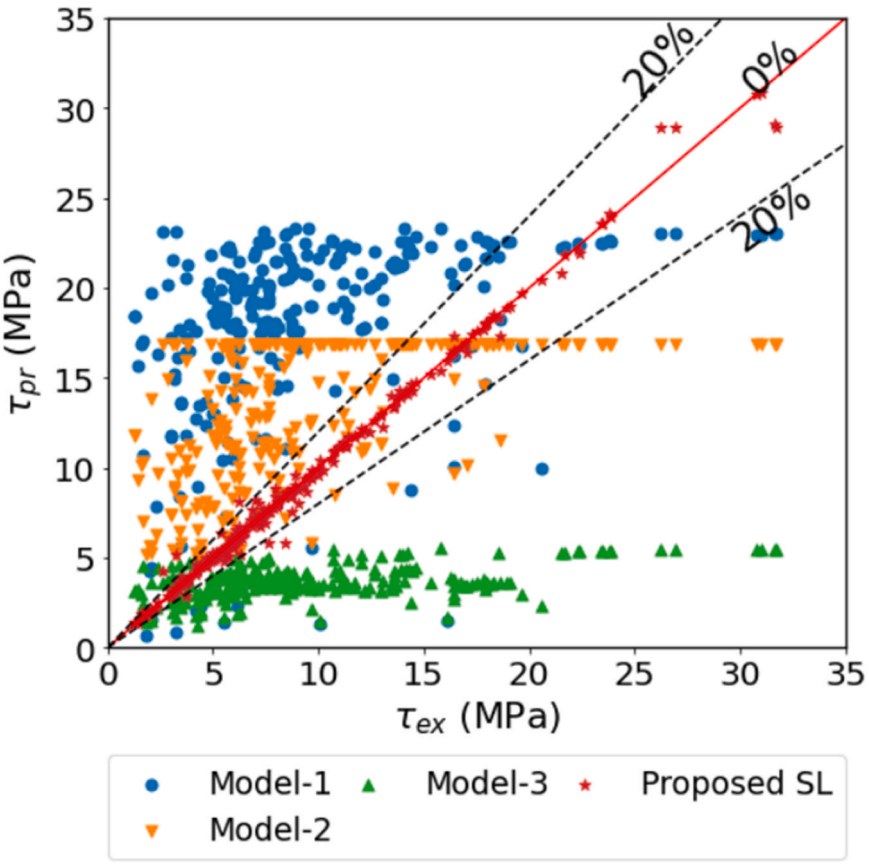

Fig. 9. Comparisons of bond strength predictions using the proposed and existing models with ± 20% error bounds.

reinforcement and pull-out specimens.

6.3. Comparison with existing analytical models

As presented above, the most accurate prediction of the bond strength between concrete and corroded steel reinforcement was obtained by the SL model. Hence, to evaluate the feasibility and efficacy of this model in practical applications, the prediction performance of the proposed SL model was further assessed against the existing analytical formulations, which are provided in Section 2. As previously discussed, the model of Cabrera [11] was established for fly ash concrete. In addition, the predictive model of Chung et al. [12] was developed based on the C_L. When the C_L is 2% or less, Chung et al. [12] assumed a constant bond strength of 16.87 MPa, whereas when the $C_L$is higher than 2%, the bond strength could be estimated as $24.7C_L{}^{-0.55}$. Furthermore, Stanish et al. [44] model is based on compressive strength and C_L. The experimental bond strength versus the predicted bond strength based on the current analytical models is demonstrated in Fig. 8. Throughout the discussion, Models 1, 2, and 3 refer to Cabrera [11], Chung et al. [12], and Stanish et al. [44] models, respectively. As can be seen in Fig. 8, most of the predictions were significantly overestimated by Model 1, implying that Model 1 is unsafe for predicting the bond strength of concrete with steel reinforcement under corrosive conditions. The inaccuracy of the model's prediction could be due to the incorporation effect of fly ash, which impedes the chloride movement and, in turn, prevents the loss of the bond strength due to corrosion [11]. Moreover, this model fails to consider other important factors that influence the bond strength such as steel yield strength, compressive strength of concrete, reinforcement type, c_c/d_b ratio, d_b/l_b ratio, and test type. Similarly, inconsistent predictions were observed in Model 2, as

Table 5
Performance of different bond strength models.

Model		MAE (MPa)	MAPE (%)	RMSE (MPa)	Mean of τ_{pr}/τ_{ex}	STD of τ_{pr}/τ_{ex}
Cabrera[11]	Model-1	9.31	166	10.40	2.59	1.97
Chung et al. [12]	Model-2	5.11	92.67	6.17	1.85	1.25
Stanish et al.[44]	Model-3	5.98	54.44	8.12	0.55	0.39
Proposed SL		0.27	3.72	0.52	1.01	0.078

significant proportions of the predictions were either overestimated or underestimated. The unsatisfactory predictions of Model 2 stem from its assumption of a constant bond strength of 16.87 MPa for specimens with $C_L$of 2% or less in addition to the failure to consider important factors. This assumed bond strength contradicts the compiled experimental results, where a number of specimens included in the database showed bond strength lower than 16.87 MPa. Consequently, Model 2 tends to overestimate most of its predictions. In addition, the predictions of the bond strength by Model 3 were mostly over-conservative, despite the fact that the model accounts for the concrete compressive strength and C_L. It is worth mentioning that all models failed to consider important factors that influence the bond strength of concrete in corrosive environments. Particularly, Model 1 and Model 2 failed to consider important factors such as steel yield strength, compressive strength of concrete, reinforcement type, c_c/d_b ratio, d_b/l_b ratio, and test type, while Model 3 failed to consider the effect of steel yield strength, reinforcement type, c_c/d_b ratio, d_b/l_b ratio, and test type.

Fig. 9 shows the variations between the predictive performance of the proposed SL model and the analytical models. As can be observed in the figure, the SL model was less scattered and almost all predictions were bounded within the ± 20% error margin, whereas the predictions achieved by the existing analytical models were highly overestimated or underestimated. The accuracy of the proposed SL model against the existing analytical models was also statistically analyzed in terms of the MAE, MAPE, RMSE, and mean and standard deviation (STD) of τ_{pr}/τ_{ex} ratio, as shown in Table 5 and Fig. 10. The proposed SL model decreased the RMSE by 95%, 91%, and 94% compared to Models 1, 2, and 3, respectively (Table 5). In addition, it had the lowest MAE and MAPE compared to the existing models (Fig. 10), and hence the proposed SL model appeared to be a mere line on the radar plot compared to the analytical models. The four models showed an average τ_{pr}/τ_{ex} ratios of 2.59 with STD of 1.97 for Model 1, 1.85 with STD of 1.25 for Model 2, 0.55 with STD of 0.39 for Model 3, and 1.01 with STD of 0.078 for the proposed model, as listed Table 5. This observation confirms that the proposed model has the most accurate and consistent predictions with an average ratio of 1.01 and the least STD of 0.078 (Table 5).

6.4. *Super learner-based practical bond strength prediction GUI tool*

As discussed earlier, the proposed SL model showed great potential in predicting the bond strength of concrete with corroded bars. However, it is important to develop a user-friendly tool for the practical application of the developed model. Consequently, a graphical user interface (GUI) of the proposed super leaner model is developed in Python for its practical use, as shown in Fig. 11. The developed GUI tool can be accessed at https://github.com/twakjira/GUI-prediction-tool-bond-strength-. The range of applicability of the proposed model is shown in Fig. 11. The categorical input variables (i.e., test and reinforcement types) are converted to numerical values in using the developed GUI tool. Values 1 and 2 are used for smooth and deformed bars, respectively; while values 0 and 1 are used for pull-out specimen and beam specimen, respectively, as shown in Fig. 11. The established GUI tool is used to predict the bond strength of concrete with corroded steel of Specimen B10–05 tested by [43]. As shown in Fig. 11, the predicted bond strength is 17.93 MPa, which strongly agrees with the corresponding experimental value (τ_{ex} = 17.90 MPa [43]).

7. Conclusions

The bond strength between concrete and reinforcement is vital for the composite action and serviceability of RC structures, yet it is notably susceptible to degradation from reinforcement bar corrosion, particularly in marine environments. Therefore, an accurate and reliable model

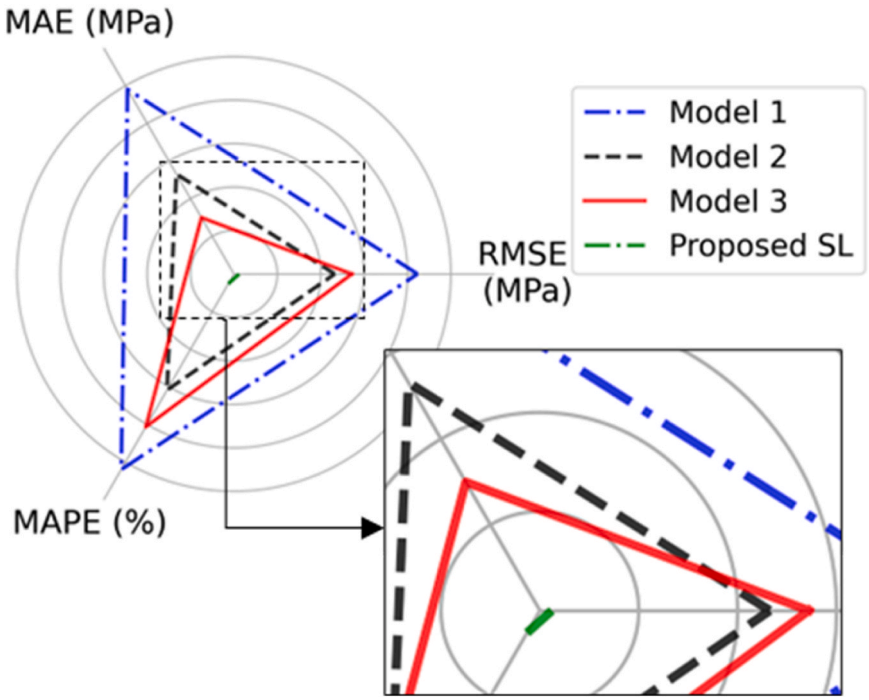

Fig. 10. Performance comparison of proposed and existing models on the complete dataset.

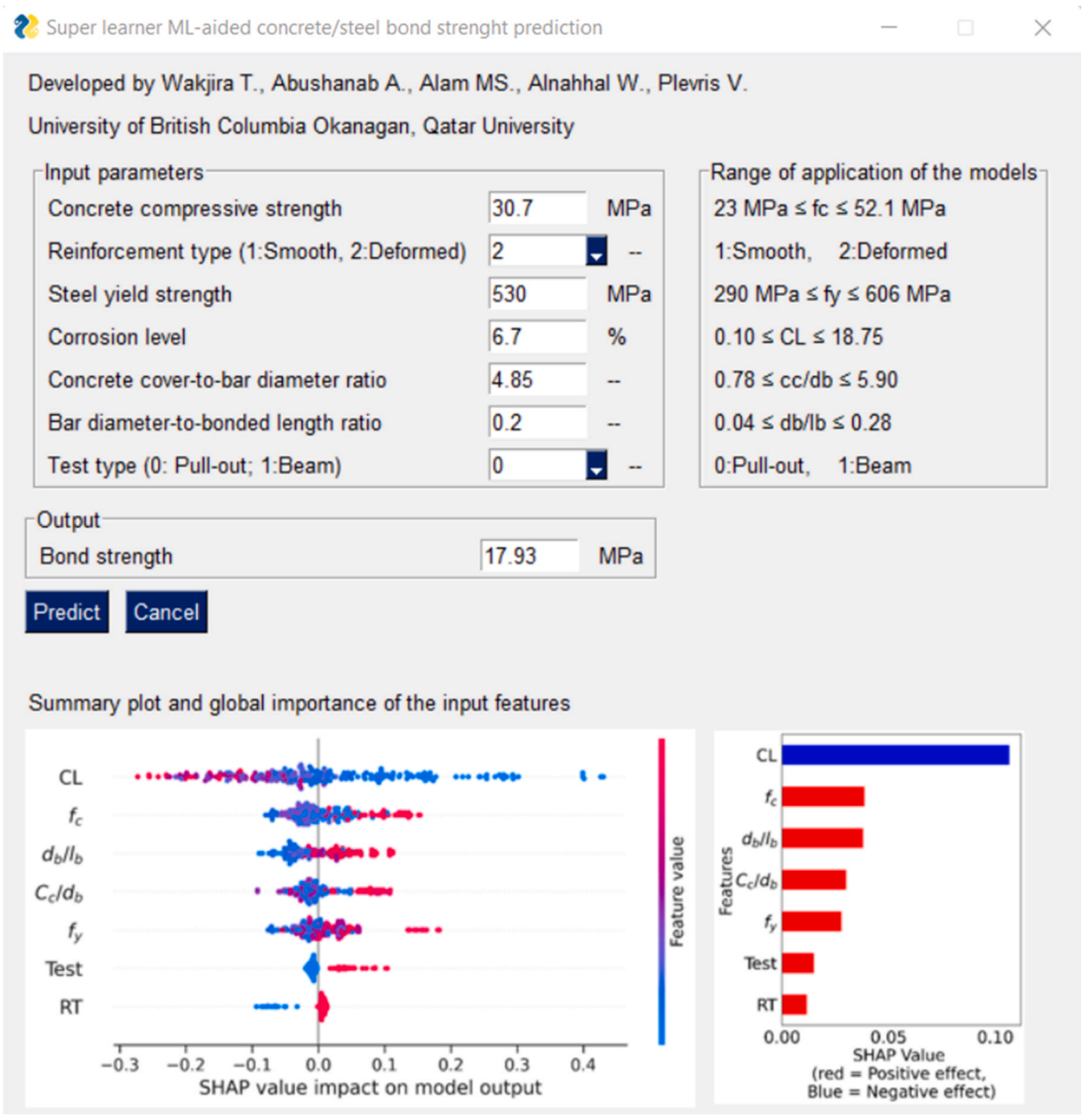

Fig. 11. GUI tool of the proposed super learner and bond strength prediction for Specimen B10–05 of Ref. [43].

for assessing bond strength in corrosive settings is essential to accurately evaluate the serviceability and structural integrity of corroded RC structures. To this end, this study developed explainable ML models for accurately predicting the bond strength of concrete and corroded reinforcement. A total of eight ML predictive models were developed using a comprehensive database of 249 experiments to evaluate the bond strength between concrete and corroded steel bars. A total of seven factors were considered, namely C_L, steel yield strength, compressive strength of concrete, c_c/d_b, d_b/l_b, reinforcement type, and test type. Moreover, the predictive accuracy of the proposed SL model was evaluated against existing analytical models. The SHAP technique was also employed to rank the input parameters and explain their impact on the bond strength of concrete and corroded reinforcement. The main conclusions of the study can be summarized below:

1. The least accurate predictive single model, KRR, was associated with an R^2 of 67.9% on the test sets. The CART model had the highest accurate predictions among the single models with an R^2, RRMSE, and KGE of 97%, 0.22 MPa, and 90.5% on the test set, respectively.
2. The ensemble of CART in boosting models, ADB, GBT, xgBoost, improved the accuracy of the single models. The R^2 of all ensemble models were greater than 94%, indicating the benefits of ensemble models. Moreover, the SL model further improved the prediction accuracy of the models by integrating the predictions from the CART, GBT, and xgBoost.
3. A comparison between the proposed super learner model and existing analytical models showed that the SL model had the most accurate and reliable prediction of the bond strength with an average τ_{pr}/τ_{ex} ratio 1.01 with a standard deviation of 0.078.
4. According to SHAP analysis results, C_L is the most influential factor on the bond strength, followed by concrete compressive strength, d_b/l_b, c_c/d_b, steel yield strength, test type, and reinforcement type. Moreover, the C_L showed a negative effect, whilst other parameters showed positive effects. Thus, an increase in all factors except C_L increases the bond strength.
5. A user-friendly GUI tool was also developed based on the proposed SL model, which facilitates practical implementation and accurate prediction of bond strength between concrete and steel reinforcement in corrosive environments.

In summary, this study demonstrated the effectiveness of using ML models to predict the bond strength of concrete and corroded reinforcement bars. However, the applicability of the developed model as well as the resulting GUI tool are limited to the range of the factors considered during model development. For instance, the compressive strength of concrete, yield strength of steel, and corrosion level are limited to the respective values of 52.10 MPa, 606 MPa, and 18.75%. Therefore, future studies are recommended to perform further experimental tests to widen the data in the literature and cover specimens with high and ultra-high-performance concrete, high-strength steel reinforcement, and higher corrosion levels. Future research is also recommended to investigate the bond failure mode of concrete with corroded reinforcement.

Declaration of Competing Interest

The authors declare that they have no known competing financial interests or personal relationships that could have appeared to influence the work reported in this paper.

Acknowledgment

This publication was made possible by GSRA grant GSRA6-1-0509-19022 from the Qatar National Research Fund (QNRF, a member of Qatar Foundation). Also, the financial support from Qatar University through grant no. QUST-1-CENG-2020-17 is acknowledged. The findings achieved herein are solely the responsibility of the authors.

References

[1] Jiang C, Wu Y-F, Dai M-J. Degradation of steel-to-concrete bond due to corrosion. Constr Build Mater 2018;158:1073–80. https://doi.org/10.1016/j.conbuildmat.2017.09.142.
[2] Abushanab A, Alnahhal W. Bond strength of corroded reinforced recycled aggregate concrete with treated wastewater and fly ash. J Build Eng 2023;79:107778. https://doi.org/10.1016/j.jobe.2023.107778.
[3] Amleh L, Ghosh A. Modeling the effect of corrosion on bond strength at the steel–concrete interface with finite-element analysis. Can J Civ Eng 2006;33:673–82. https://doi.org/10.1139/l06-052.
[4] Abushanab A, Alnahhal W. Flexural behavior of reinforced concrete beams prepared with treated wastewater, recycled concrete aggregates, and fly ash. Structures 2022;45:2067–79. https://doi.org/10.1016/j.istruc.2022.10.029.
[5] Hoang N-D, Tran X-L, Nguyen H. Predicting ultimate bond strength of corroded reinforcement and surrounding concrete using a metaheuristic optimized least squares support vector regression model. Neural Comput Appl 2020;32:7289–309. https://doi.org/10.1007/s00521-019-04258-x.
[6] Abushanab A, Alnahhal W. Life cycle cost analysis of sustainable reinforced concrete buildings with treated wastewater, recycled concrete aggregates, and fly ash. Results Eng 2023;20:101565. https://doi.org/10.1016/j.rineng.2023.101565.
[7] Al-Sulaimani GJ, Kaleemullah M, Basunbul IA, Rasheeduzzafar. Influence of corrosion and cracking on bond behavior and strength of reinforced concrete members. Acids Struct J 1990;87. https://doi.org/10.14359/2732.
[8] Zhao Y, Lin H, Wu K, Jin W. Bond behaviour of normal/recycled concrete and corroded steel bars. Constr Build Mater 2013;48:348–59. https://doi.org/10.1016/j.conbuildmat.2013.06.091.
[9] Lin H, Zhao Y. Effects of confinements on the bond strength between concrete and corroded steel bars. Constr Build Mater 2016;118:127–38. https://doi.org/10.1016/j.conbuildmat.2016.05.040.
[10] Farhan NA, Sheikh MN, Hadi MNS. Experimental Investigation on the Effect of Corrosion on the Bond Between Reinforcing Steel Bars and Fibre Reinforced Geopolymer Concrete. Structures 2018;14:251–61. https://doi.org/10.1016/j.istruc.2018.03.013.
[11] Cabrera JG. Deterioration of concrete due to reinforcement steel corrosion. Cem Concr Compos 1996;18:47–59. https://doi.org/10.1016/0958-9465(95)00043-7.
[12] Chung L, Jay Kim J-H, Yi S-T. Bond strength prediction for reinforced concrete members with highly corroded reinforcing bars. Cem Concr Compos 2008;30:603–11. https://doi.org/10.1016/j.cemconcomp.2008.03.006.
[13] Yalciner H, Eren O, Sensoy S. An experimental study on the bond strength between reinforcement bars and concrete as a function of concrete cover, strength and corrosion level. Cem Concr Res 2012;42:643–55. https://doi.org/10.1016/j.cemconres.2012.01.003.
[14] Fu B, Chen S-Z, Liu X-R, Feng D-C. A probabilistic bond strength model for corroded reinforced concrete based on weighted averaging of non-fine-tuned machine learning models. Constr Build Mater 2022;318:125767. https://doi.org/10.1016/j.conbuildmat.2021.125767.
[15] Wakjira TG, Ebead U, Alam MS. Machine learning-based shear capacity prediction and reliability analysis of shear-critical RC beams strengthened with inorganic composites. Case Stud Constr Mater 2022;16:e01008. https://doi.org/10.1016/j.cscm.2022.e01008.
[16] Degtyarev VV, Tsavdaridis KD. Buckling and ultimate load prediction models for perforated steel beams using machine learning algorithms. J Build Eng 2022;51. https://doi.org/10.1016/j.jobe.2022.104316.
[17] Degtyarev VV, Naser MZ. Boosting machines for predicting shear strength of CFS channels with staggered web perforations. Structures 2021;34:3391–403. https://doi.org/10.1016/j.istruc.2021.09.060.
[18] Cakiroglu C, Islam K, Bekdaş G, Isikdag U, Mangalathu S. Explainable machine learning models for predicting the axial compression capacity of concrete filled steel tubular columns. Constr Build Mater 2022;356. https://doi.org/10.1016/j.conbuildmat.2022.129227.
[19] Wakjira TG, Rahmzadeh A, Alam MS, Tremblay R. Explainable machine learning based efficient prediction tool for lateral cyclic response of post-tensioned base rocking steel bridge piers. Structures 2022;44:947–64. https://doi.org/10.1016/j.istruc.2022.08.023.
[20] Abushanab A, Wakjira TG, Alnahhal W. Machine Learning-Based Flexural Capacity Prediction of Corroded RC Beams with an Efficient and User-Friendly Tool. Sustainability 2023;15:4824. https://doi.org/10.3390/su15064824.
[21] Wakjira TG, Abushanab A, Ebead U, Alnahhal W. FAI: Fast, accurate, and intelligent approach and prediction tool for flexural capacity of FRP-RC beams based on super-learner machine learning model. Mater Today Commun 2022;33:104461. 10.1016/j.mtcomm.2022.104461.
[22] Nariman N, Hamdia K, Ramadan A, Sadaghian H. Optimum Design of Flexural Strength and Stiffness for Reinforced Concrete Beams Using Machine Learning. Appl Sci 2021;11:8762. https://doi.org/10.3390/app11188762.
[23] Tariq M, Khan A, Ullah A, Shayanfar J, Niaz M. Improved Shear Strength Prediction Model of Steel Fiber Reinforced Concrete Beams by Adopting Gene Expression Programming. Mater (Basel) 2022;15:3758. https://doi.org/10.3390/ma15113758.
[24] Solhmirzaei R, Salehi H, Kodur V, Naser MZ. Machine learning framework for predicting failure mode and shear capacity of ultra high performance concrete beams. Eng Struct 2020;224:111221. https://doi.org/10.1016/j.engstruct.2020.111221.
[25] Zhang Y, Burton HV. Pattern recognition approach to assess the residual structural capacity of damaged tall buildings. Struct Saf 2019;78:12–22. https://doi.org/10.1016/j.strusafe.2018.12.004.
[26] Wakjira TG, Ibrahim M, Ebead U, Alam MS. Explainable machine learning model and reliability analysis for flexural capacity prediction of RC beams strengthened in flexure with FRCM. Eng Struct 2022;255. https://doi.org/10.1016/j.engstruct.2022.113903.
[27] Cakiroglu C, Islam K, Bekdaş G, Kim S, Geem ZW. Interpretable machine learning algorithms to predict the axial capacity of FRP-reinforced concrete columns. Materials 2022;15. https://doi.org/10.3390/ma15082742.
[28] Cakiroglu C, Bekdaş G, Kim S, Geem ZW. Explainable ensemble learning models for the rheological properties of self-compacting concrete. Sustainability 2022;14:14640. https://doi.org/10.3390/su142114640.
[29] Degtyarev VV. Machine learning models for predicting bond strength of deformed bars in concrete. Acids Struct J 2022;119:43–56. https://doi.org/10.14359/51734833.
[30] Wang X., Liu Y., Xin H. Bond strength prediction of concrete-encased steel structures using hybrid machine learning method. Structures 2021;32:2279–2292. https://doi.org/10.1016/j.istruc.2021.04.018.
[31] Dahou Z, Mehdi Sbartaï Z, Castel A, Ghomari F. Artificial neural network model for steel–concrete bond prediction. Eng Struct 2009;31:1724–33. https://doi.org/10.1016/j.engstruct.2009.02.010.
[32] Golafshani EM, Rahai A, Sebt MH, Akbarpour H. Prediction of bond strength of spliced steel bars in concrete using artificial neural network and fuzzy logic. Constr Build Mater 2012;36:411–8. https://doi.org/10.1016/j.conbuildmat.2012.04.046.
[33] Orangun CO, Jirsa JO, Breen JE. A reevaulation of test data on development length and splices. In Journal Proceedings 1977;74(3):114–22.
[34] Darwin D, McCabe SL, Idun EK, Schoenekase SP. Development length criteria. Bars not confined by transverse reinforcement. Acids Struct J 1992;89:709–20.
[35] Almusallam AA, Al-Gahtani AS, Aziz AR, Rasheeduzzafar. Effect of reinforcement corrosion on bond strength. Constr Build Mater 1996;10:123–9. https://doi.org/10.1016/0950-0618(95)00077-1.
[36] Auyeung Y, Balaguru P, Chung L. Bond behavior of corroded reinforcement bars. Acids Mater J 2000;97. https://doi.org/10.14359/826.
[37] H. Shima. Local bond stress-slip relationship of corroded steel bars embedded in concrete Proc Third Int Symp Bond Concr Bp 2002 153 158.(p).
[38] Zhao Y, Jin W. Test study on bond behavior of corroded steel bars and concrete. J-Zhejiang Univ Eng Sci 2002;36:352–6.
[39] Fang C, Lundgren K, Chen L, Zhu C. Corrosion influence on bond in reinforced concrete. Cem Concr Res 2004;34:2159–67. https://doi.org/10.1016/j.cemconres.2004.04.006.
[40] G. Horrigmoe, I. Saether, R. Antonsen, B. Arntsen, Lab Investig Steel Bar Corros Concr: Sustain Bridges Backgr Doc 10 2007 SB3.
[41] Wu Y-Z, Lv H-L, Zhou S-C, Fang Z-N. Degradation model of bond performance between deteriorated concrete and corroded deformed steel bars. Constr Build Mater 2016;119:89–95. https://doi.org/10.1016/j.conbuildmat.2016.04.061.
[42] Coccia S, Imperatore S, Rinaldi Z. Influence of corrosion on the bond strength of steel rebars in concrete. Mater Struct 2016;49:537–51. https://doi.org/10.1617/s11527-014-0518-x.
[43] Mak MWT, Desnerck P, Lees JM. Corrosion-induced cracking and bond strength in reinforced concrete. Constr Build Mater 2019;208:228–41. https://doi.org/10.1016/j.conbuildmat.2019.02.151.

[44] Stanish K, Hooton RD, Pantazopoulou SJ. Corrosion effects on bond strength in reinforced concrete. Acids Struct J 1999;96:915–21.
[45] Yu H, Kim SSVM. tutorial-classification, regression and ranking. Handb Nat Comput 2012;1–4:479–506. https://doi.org/10.1007/978-3-540-92910-9_15.
[46] Freund Y, Schapire RE. A decision-theoretic generalization of on-line learning and an application to boosting. J Comput Syst Sci 1997;55:119–39. https://doi.org/10.1006/jcss.1997.1504.
[47] T. Chen C. Guestrin Xgboost: A scalable tree boosting system 22nd SIGKDD Conf Knowl Discov Data Min 2016.
[48] Laan MJ, Van Der, Polley EC, Hubbard AE. Super learner. Stat Appl Genet Mol Biol 2007;6. https://doi.org/10.2202/1544-6115.1309.
[49] Plevris V., Solorzano G., Bakas N., Ben Seghier M. Investigation of performance metrics in regression analysis and machine learning-based prediction models. ECCOMAS Congr. 2022 - 8th Eur. Congr. Comput. Methods Appl. Sci. Eng., 2022. https://doi.org/10.23967/eccomas.2022.155.
[50] Lundberg S.M., Lee S. A Unified Approach to Interpreting Model Predictions. 31st Conf. neural Inf. Process. Syst. (NIPS 2017), Long Beach, CA, USA: 2017, p. 1–10.